Original Article | Journal of Biosystems Engineering

J. of Biosystems Eng. 39(4):310-317. (2014. 12)
http://dx.doi.org/10.5307/JBE.2014.39.4.310

eISSN : 2234-1862
pISSN : 1738-1266

Analysis of Airflow Pattern in Plant Factory with Different Inlet and Outlet Locations using Computational Fluid Dynamics

Tae-Gyu Lim[1], Yong Hyeon Kim[2]

[1]*Department of Bioindustrial Machinery Engineering, Graduate School, Chonbuk National University, Jeonju, Korea*
[2]*Department of Bioindustrial Machinery Engineering, College of Agriculture & Life Sciences, Chonbuk National University, Jeonju, Korea (Institute of Agricultural Science & Technology)*

Received: October 12nd, 2014; Revised: October 27th, 2014; Accepted: November 17th, 2014

Abstract

Purpose: This study was conducted to analyze the air flow characteristics in a plant factory with different inlet and outlet locations using computational fluid dynamics (CFD). **Methods:** In this study, the flow was assumed to be a steady-state, incompressible, and three-dimensional turbulent flow. A realizable k-ε turbulent model was applied to show more reasonable results than the standard model. A CFD software was used to perform the numerical simulation. For validation of the simulation model, a prototype plant factory (5,900 mm x 2,800 mm x 2,400 mm) was constructed with two inlets (Φ250 mm) and one outlet (710 mm x 290 mm), located on the top side wall. For the simulation model, the average air current speed at the inlet was 5.11 $m \cdot s^{-1}$. Five cases were simulated to predict the airflow pattern in the plant factory with different inlet and outlet locations. **Results:** The root mean square error of measured and simulated air current speeds was 13%. The error was attributed to the assumptions applied to mathematical modelling and to the magnitude of the air current speed measured at the inlet. However, the measured and predicted airflow distributions of the plant factory exhibited similar patterns. When the inlets were located at the center of the side wall, the average air current speed in the plant factory was increased but the spatial uniformity was lowered. In contrast, if the inlets were located on the ceiling, the average air current speed was lowered but the uniformity was improved. **Conclusions:** Based on the results of this study, it was concluded that the airflow pattern in the plant factory with multilayer cultivation shelves was greatly affected by the locations of the inlet and the outlet.

Keywords: Airflow, Computational fluid dynamics (CFD), Plant factory, Turbulent model

Introduction

As an alternative to fluctuating agricultural production due to abnormal climate conditions, plant factories with artificial lighting sources have been recently used for commercial production of leafy vegetables (Kozai, 2013). Since the environments inside the plant factory can be optimally controlled, the use of plant factory has gradually increased to include propagation, grafting, and transplant production of horticultural crops. In addition, multilayer shelves equipped with hydroponic culture beds have been extensively adopted for increasing the space utilization of the plant factory. These shelves are required for healing and acclimation of grafted seedlings as well as cultivation of leafy vegetables, herbs, medicinal plants, and others, with a height of 30 cm or less. However, the uniformity of the physical environment such as the air temperature and humidity in the plant factory can be lowered owing to the increased number of layers of cultivation shelves, the increased resistance to airflow by plants, and the excessive heat generated from the artificial lighting sources (Kim and Kozai, 1996; Park et al., 2011). Unlike many prior studies that have been conducted in the greenhouse and livestock houses on ventilation characteristics, studies on the airflow pattern of the plant factory are still lacking.

***Corresponding author:** Yong Hyeon Kim
Tel: +82-63-270-2618; **Fax:** +82-63-270-2620
E-mail: yhkim@jbnu.ac.kr

The primary reason for the lack of relevant studies is the fact that the plant factory has not been widely utilized in the field of agriculture. Therefore, prior to designing the plant factory, the analysis of the airflow characteristics constitutes a very important task to improve the uniform distribution of air temperature and humidity.

Locations and sizes of the inlet and outlet, and air current speed from the inlet are very important elements for the environmental management of closed plant production system. Particularly, the overall airflow characteristics can be greatly affected by the locations of the inlet and the outlet. Previous studies on the airflow pattern of a closed space in the shape of a box, with different locations and sizes of the inlet and the outlet, have reported the obvious difference in airflow characteristics (Choi and Cho, 2009; Kim et al., 2010). However, cost and time are required for attaining meaningful results that correspond to the optimal effect of the design parameters on the airflow pattern in greenhouses or plant factory, such as locations, sizes, and airflow rate based on repeated experiments.

Numerical analyses based on computational fluid dynamics (CFD) can predict and analyze the airflow characteristics of the model that are difficult to be analyzed by experiments (Yun, 2002). CFD was introduced in the 1970s but it began to be used in the agriculture in the 1990s owing to the rapid development of computer performance (Lee, 2013). Studies analyzing the airflow characteristics of the plant factory using CFD have been increasing recently; however, published results have targeted a particular plant factory type. It is therefore difficult to allow extrapolation of findings to other types of plant factories. In accordance to recent research trends the airflow characteristics of the vertical plant factory has been studied to reduce the temperature deviation between the top and bottom surfaces using CFD simulations. Subsequently, the effect of the locations of the inlet and the exhaust fan on the air flow characteristics in agricultural buildings was analyzed by Lee (2013). Additionally, a numerical study was performed for assessment of the thermal environment of the vertical plant factory based on natural light that analyzed the effects of the air temperature and volume supply (Park et al., 2013). The objectives of this study were to analyze the air flow characteristics in the plant factory with different inlet and outlet locations using CFD.

Materials and Methods

Experimental plant factory

For validation of the simulation model, a prototype plant factory was constructed (Figure 1). The internal dimensions of the constructed plant factory manufactured were 5,900 mm x 2,800 mm x 2,400 mm. Two inlets (Φ250 mm) and one outlet (710 mm x 290 mm) were located on the top side wall. The wall used a heat insulating material with a thickness of 100 mm. The dimensions of each of the five cultivation shelf layers were 1,700 mm x 635 mm x 1,800 mm and the inter-layer spacing was 265 mm. The multilayer cultivation shelves were arranged symmetrically, as shown in Figure 1.

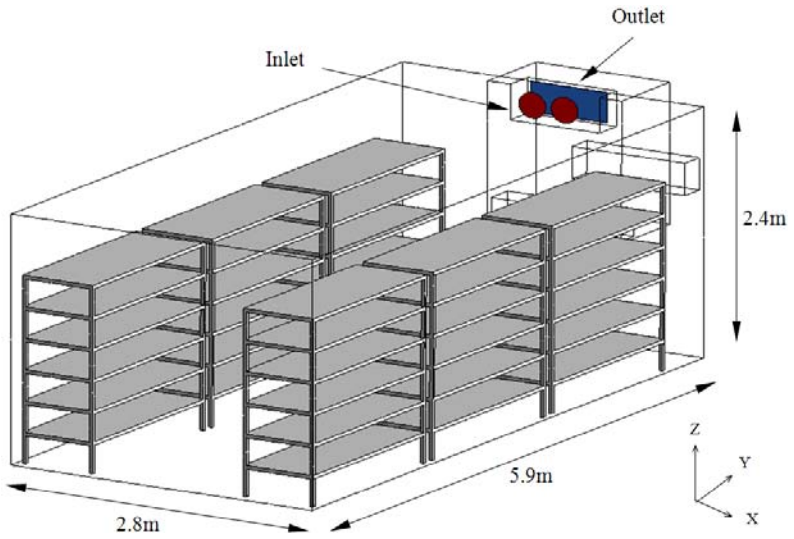

Figure 1. A schematic diagram of the plant factory quipped multilayer cultivation shelves (Case 1).

Numerical simulation

In this study, the fluid flow in the analysis region was assumed to be a steady-state, incompressible, and three-dimensional turbulent flow. The numerical calculation of the airflow is generally based on the conservation equations of aerodynamics on (1) mass, (2) momentum, and (3) energy (Boulard and Wang, 2002). However, radiative transfer, thermal conductivity, and thermal buoyancy were ignored because the heating elements were not considered. Therefore, the energy conservation equation was not used. A realizable *k-ε* turbulent model was used in this analysis to show more reasonable results compared to the standard model in other fields of flow analysis.

$$\frac{\partial_\rho}{\partial_t}+\frac{\partial}{\partial x_i}(\rho v_i)=s_m \tag{1}$$

$$\frac{\partial_\rho}{\partial_t}+\frac{\partial}{\partial x_j}(\rho v_i v_j)=\frac{\partial \tau_{ij}}{\partial x_j}-\frac{\partial P}{\partial x_i}+s_i \tag{2}$$

$$\frac{\partial}{\partial_t}(\rho c_p T)+\frac{\partial}{\partial x_i}(u_i \rho c_p T)=\frac{\partial}{\partial x_i}\left(k\frac{\partial T}{\partial x_i}\right)+S_h \tag{3}$$

where *u* and v are the components of velocity vector, *i* and *j* are the corresponding directional vectors, *t* is the time, ρ is the density, P is the pressure, τ_{ij} is the stress tensor, T is the temperature, c_p is the specific heat, k is the thermal conductivity, *x* is the Cartesian space coordinate, S_m is the mass generated per unit volume, and S_h is the energy per unit volume. Externally applied body and surface forces, such as gravity for example, are represented by s_i.

$$\frac{\partial}{\partial_t}(\rho k)+\frac{\partial}{\partial x_j}(\rho k u_j) = \frac{\partial}{\partial x_j}\left[\left(\mu+\frac{\mu_t}{\sigma_k}\right)\frac{\partial}{k\partial x_j}\right]+G_k+G_b-\rho\varepsilon-Y_M \tag{4}$$

$$\frac{\partial}{\partial_t}(\rho \varepsilon)+\frac{\partial}{\partial x_j}(\rho \varepsilon u_j) = \frac{\partial}{\partial x_j}\left[\left(\mu+\frac{\mu_\varepsilon}{\sigma_\varepsilon}\right)\frac{\partial_\varepsilon}{\partial x_j}\right]+\rho C_1 S\varepsilon-\rho C_2\frac{\varepsilon^2}{k+\sqrt{\nu\varepsilon}}+C_{1\varepsilon}\frac{\varepsilon}{k}C_{3\varepsilon}G_b \tag{5}$$

The employed *k-ε* turbulence model is a two-equation model, comprising the turbulence kinetic energy equation (4) and the turbulent kinetic energy dissipation equation (5), where k is the turbulent kinetic energy, ε is the turbulent dissipation rate, $\rho\varepsilon$ is the viscous dissipation, Y_M is the attenuation and expansion caused by compressibility effects, *S* is turnover ratio, ν is the kinematic coefficient of viscosity, μ is the coefficient of viscosity, G_k and G_b are the turbulent kinetic energies owing to the average flow field and buoyancy, respectively, σ_k and σ_ε are the Prandtl number of turbulent kinetic energy and the turbulent dissipation rate, respectively, and C_1, C_2, C_3 are constants determined experimentally. The quantitative values of the model parameters are as follows (Shih et al., 1995). $C_1=\max\left[0.43,\frac{\eta}{\eta+5}\right]$, $\eta=S\frac{k}{\varepsilon}$, $S=\sqrt{2S_{ij}S_{ij}}$, $C_{1\varepsilon}=1.44$, $C_2=1.9$, $\sigma_k=1.0$, and $\sigma_\varepsilon=1.2$. The CFD software ANSYS (FLUENT 13, ANSYS, USA) was used to perform the numerical simulation.

In the simulation setup step for the selection of a solution method, the 'SIMPLE' algorithm for pressure-velocity coupling was selected. In addition, the 'PRESTO' technique was applied. This technique is advantageous to flow analysis that is associated with rapid pressure changes for discretization of the pressure term. Additionally, the second order upwind difference scheme was applied for the discretization.

The model was designed to be the same as the constructed plant factory, using CATIA (V5, Dassault Systemes, France). A flow model was constructed by removing the shelves from an internal structure model of the rectangular body, and subsequent application to a non-uniform grid. The grid constructed in this study was approximately 2.7 million.

Boundary conditions

Inlet and outlet boundary conditions for the numerical solution were set up using the 'Velocity-inlet' and 'Pressure-outlet'. The air temperature of the inlet was controlled at 24°C. The average air current speed at the inlet of the simulation model was 5.11 m·s^{-1}. This value was measured at nine points located 20 cm apart from the inlet's center,

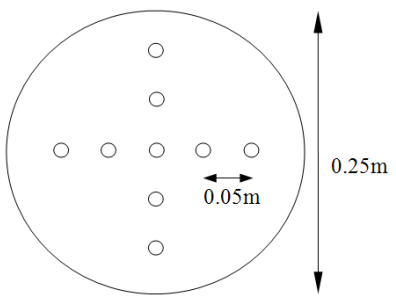

Figure 2. Locations of the airflow sensors used for measuring the air current speed at the inlet.

using an airflow sensor (Model 0965 KANOMAX, JAPAN) and a transducer (Model 6332, KANOMAX, JAPAN) (Figure 2).

To determine the proper location of the inlet and the outlet for effective air circulation, five cases were simulated in this study (Figure 3). The location of the inlet for each case was set to be at the center of the plant factory to avoid a direct impact of a high pressure wind outflow from the inlet. Case 1 is a model of the experimental plant factory (Figure 1). Case 2 is a model in which the outlet is placed on the ceiling opposite to the inlet, at the center of the side wall. Unlike other cases, case 3 is a model that uses two outlets that are located on the side wall to induce internal circulation along the center aisle. Cases 4 and 5 are models that consider the updraft and downdraft from the ceiling.

To validate the simulation model, the measured air current speed of case 1 was used for comparisons with the simulated results. Subsequently, the air current speeds for cases 2-5 were predicted using the simulation model.

The air current speeds used for validation were measured

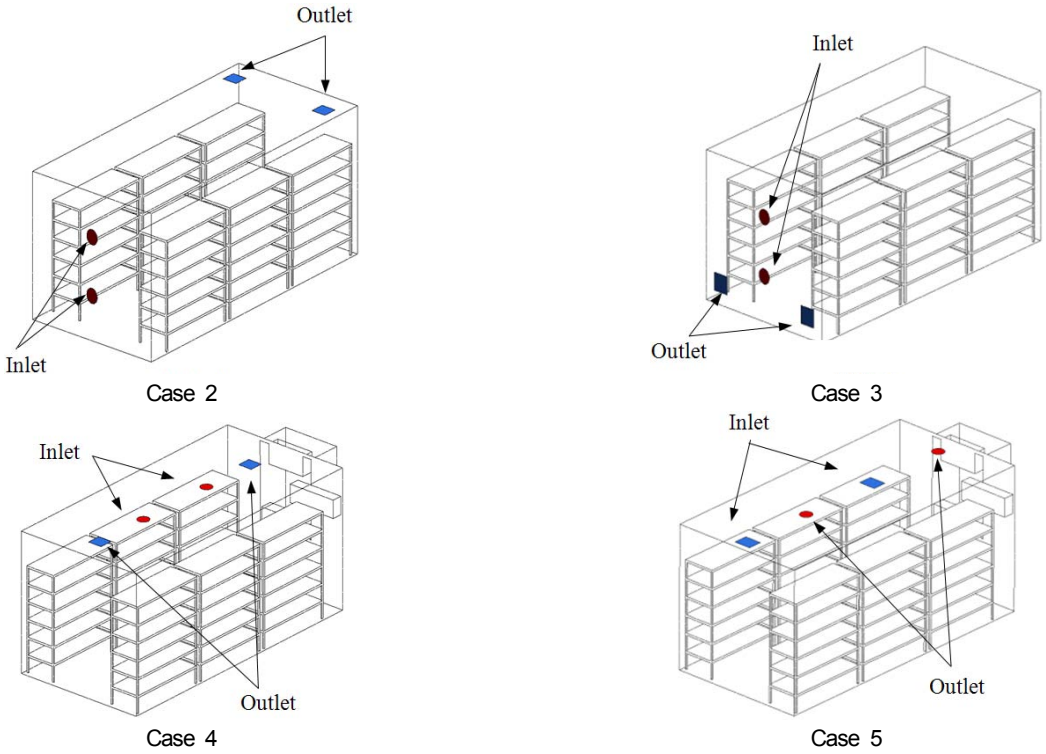

Figure 3. Four simulated cases with different locations of the inlet and outlet.

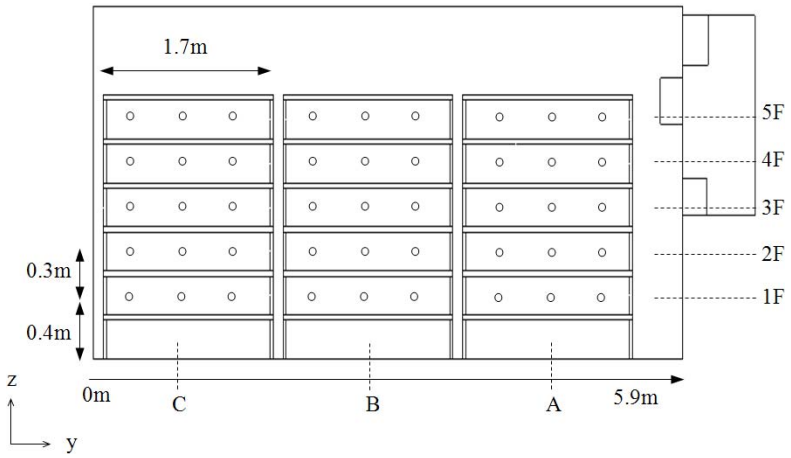

Figure 4. Locations of the airflow sensors used for measuring the air current speed at the y-z plane and at x = 2.425 m.

using three airflow sensors and transducers located 10 cm above each shelf layer. The average air current speed was obtained from data measured over a period of 10 minutes. The locations of the anemometers used for measuring the air current speed in the plant factory are indicated using the labels A-C and 1F-5F, as shown in Figure 4. In this study, the uniformity was defined as the deviations of the simulated air current speed for cases 1-5 to the value for case 1 (Kwon et al., 2010). Moreover, in this study, the root mean square error for comparing the measured and simulated values was defined in accordance to the following equation:

$$RMS = \sqrt{\frac{1}{n}\sum_{i=1}^{n}\left(y_i - \hat{y_i}\right)^2} \quad (6)$$

where y_i refers to the measured values, $\hat{y_i}$ refers to the simulated values, and *n* refers to the sample number.

Results and Discussion

Validation of simulation model

Table 1 shows the results obtained by comparing the air current speed measured by the airflow sensors and the corresponding simulated value. The RMS error of the measured and simulated results was 13%. The difference in the air current speed between the simulated and the measured values increased with a decreasing distance from the inlet of the airflow. This result was attributed to the assumptions applied for the simplifications of mathematical modelling and to the magnitude of the air current speed measured at the inlet. In particular, the air current speed at the top and bottom sides of the cultivation shelves was overestimated. The highest air current speed value recorded for both results occurred around shelves B and C. This is because the air discharged from the inlet reached the other side of the wall by flowing along the ceiling with less energy loss, based on the Coanda effect

Table 1. Comparison of air current speeds measured by the anemometers and simulated using CFD according to the different sensor locations (A-C, 1F-5F) of the cultivation shelves for case 1

Treatment		Air current speed ($m \cdot s^{-1}$)						
		1F	2F	3F	4F	5F	Mean	Average
Simulated	A	0.31	0.30	0.17	0.12	0.36	0.25	0.16±0.05
	B	0.58	0.48	0.25	0.19	0.52	0.41	
	C	0.44	0.44	0.39	0.31	0.38	0.39	
Measured	A	0.17	0.09	0.18	0.14	0.24	0.16	0.10±0.03
	B	0.52	0.20	0.21	0.33	0.46	0.34	
	C	0.44	0.33	0.17	0.25	0.38	0.32	

Table 2. Comparison of simulated air current speed according to the height and location of the cultivation shelves for cases 2-5

Treatment		Air current speed ($m \cdot s^{-1}$)						
		1F	2F	3F	4F	5F	Mean	Average
Case 2	A	0.34	0.34	0.26	0.27	0.39	0.32	0.32±0.18
	B	0.61	0.55	0.53	0.49	0.45	0.53	
	C	0.14	0.09	0.09	0.10	0.12	0.11	
Case 3	A	0.33	0.49	0.50	0.35	0.37	0.41	0.37±0.19
	B	0.51	0.57	0.61	0.56	0.55	0.56	
	C	0.09	0.12	0.13	0.14	0.15	0.13	
Case 4	A	0.18	0.11	0.09	0.10	0.38	0.17	0.13±0.07
	B	0.08	0.11	0.09	0.11	0.10	0.10	
	C	0.18	0.14	0.12	0.12	0.11	0.13	
Case 5	A	0.25	0.27	0.17	0.10	0.09	0.18	0.14±0.06
	B	0.20	0.13	0.09	0.06	0.10	0.12	
	C	0.12	0.12	0.10	0.10	0.13	0.12	

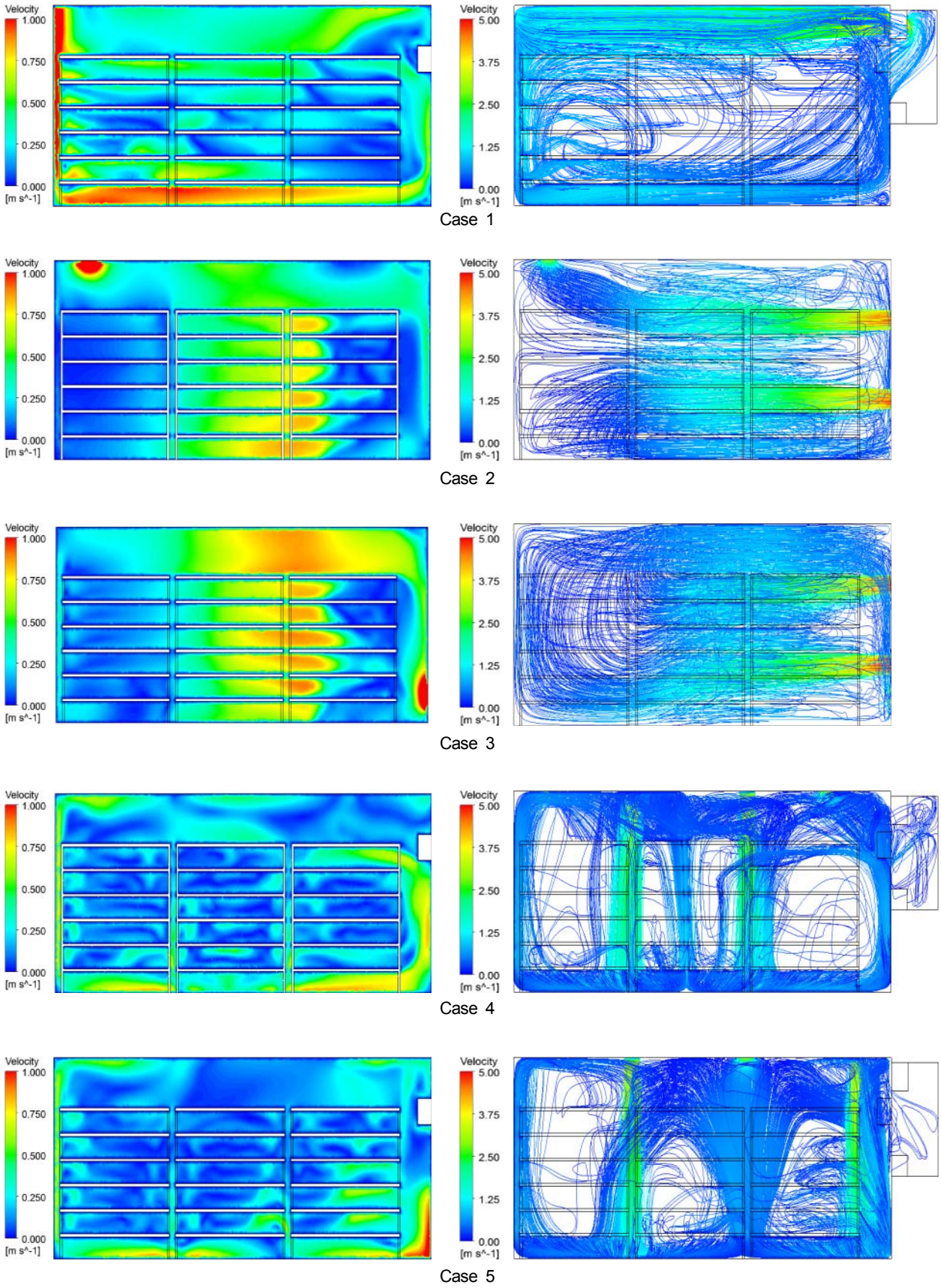

Figure 5. Airflow distribution at the y-z plane and at x = 2.425 m for the five studied cases.

(Yun et al., 2007).

However, the airflow distributions measured and predicted for case 1 exhibited a similar pattern and varied in accordance to the height and location of the shelves. Thus, the numerical simulation developed in this study was subsequently used to predict the air current speed for cases 2-5.

Effect of different locations of the inlet and outlet on the distribution of air current speed in the plant factory

Table 2 lists the analysis results for each studied case and Figure 5 depicts the air current speed distribution at the y-z plane and at x = 2.425 m. For case 2, a higher air current speed was found around shelf B. In contrast, the air current speed was lower around shelf C, at locations far from the inlet. Cases 2 and 3 exhibited a very similar pattern of airflow formation in the model for the plant factory. The average air current speeds for cases 2 and 3 were 0.32 $m \cdot s^{-1}$ and 0.37 $m \cdot s^{-1}$, respectively. They were both and higher in value than those for cases 4 and 5. Differences in the maximum and minimum air current speeds for cases 2 and 3 were both 0.52 $m \cdot s^{-1}$. These values were higher than corresponding values for other cases and constituted the primary factor that led to a lower uniformity of the air current speed in a plant factory with multilayer cultivation shelves.

Because of the swirling airflow around shelf B, the airflow could not sufficiently reach shelf A, and the uniformity of the airflow pattern was consequently lowered. Case 3 was expected to contribute to an internal air circulation along the center aisle. However, the uniformity of the air current speed was lowered significantly due to the swirling airflow around shelf B. The average of the air current speed for case 4 was 0.13 $m \cdot s^{-1}$ and was the lowest among all the treatments. The air flow pattern for case 5 was similar to that of case 4. The deviations of the average air current speed for these two cases were 0.07 $m \cdot s^{-1}$ and 0.06 $m \cdot s^{-1}$, respectively, and the differences in the maximum and minimum air current speed were 0.30 $m \cdot s^{-1}$ and 0.19 $m \cdot s^{-1}$, respectively. These results showed that the uniformity of the airflow pattern for cases 4 and 5 was fairly improved. The distributions of the air current speed for cases 2 and 3 were almost the same. Furthermore, a similar air flow pattern was also observed for cases 4 and 5. It was reported previously that the optimum air current speed for the growth of horticultural crops, such as plug seedlings, was 0.7-0.9 $m \cdot s^{-1}$ (Kim and Kozai, 1997; Kim, 1998). In comparison to such reports, the average air current speed simulated in this study was very low. Therefore, additional studies must be performed to improve the distribition of air current speed in the plant factory with different locations of inlet and outlet. From these results, it was concluded that the airflow characteristics in the closed plant factory with multilayer cultivation shelves were greatly affected by the locations of the inlet and the outlet.

Conclusions

A numerical simulation using CFD was performed to analyze the effect of different inlet and outlet locations on the air flow pattern in the plant factory with multilayer cultivation shelves. Even though the predicted magnitude of the air current speed was overestimated compared to the measured value, the flow patterns were similar. When the inlets were located at the center of the side wall, such as the cases 2-3, the average air current speed in the plant factory was increased but the uniformity was lowered. On the contrary, if the inlets were located on the ceiling, the average air current speed was lowered but the uniformity was improved. Since the average predicted air current speed was low, additional studies were required to improve the distribition of the air current speed in the plant factory using different locations of the inlet and the outlet. Based on these reported results, it was concluded that the airflow pattern in the plant factory with multilayer cultivation shelves was greatly affected by the locations of the inlet and the outlet.

Conflict of Interest

No potential conflict of interest relevant to this article was reported.

Acknowledgements

This study was performed with the support of the "Cooperative Research Program for Agriculture Science & Technology Development (Project No. PJ009466)" Rural Development Administration, Republic of Korea.

References

Boulard, T. and S. Wang. 2002. Experimental and numerical studies on the heterogeneity of crop transpiration in a plastic tunnel. J. Computers and Electronics in Agriculture 34:173-190.

Choi, J.M. and S.W. Cho. 2009. A study on the indoor airflow pattern by changing the location of mechanical terminal unit. J. of Air-Conditioning and Refrigerating 21(3):193-200 (In Korean).

Kwon, K.S., I.B. Lee, H.S. Hwang, J.P. Biotg, S.W. Hong, I.H. Seo, J.S. Choi, S.H. Song and O.G. Moon. 2010. Analysis on the optimum location of a wet air cleaner in a livestock house using CFD technology. J. of the Korean Society of Agricultural Engineers 52(3):19-29 (In Korean).

Kim, H.J., Y.I. Kim and K.S. Chung. 2010. Effect of location and size of the inlet and outlet diffusers on ventilation flow rate of a box type space. Proceedings of the SAREK(Spring) pp.311-316 (In Korean).

Kim, Y.H. 1998. Effects of air current speeds on the growth of eggplant plug seedlings in a wind tunnel under artificial lighting. J. of Bioproduction Facility and Environment 7(1):9-14 (In Korean).

Kim, Y.H. and Kozai, T. 1996. Effects of air current speed on the microclimates of the plug stand under artificial light. J. of Bioproduction Facility and Environment 5(2):160-166 (In Korean).

Kim. Y.H. and Kozai, T. 1997. Measurement of net photosynthetic rate in the plug stand. J. of Agricultural Machinery 22(3):311-316 (In Korean).

Kozai, T. 2013. Plant factory in Japan – Current situation and perspectives. Chronica Horticulturae 53(2):9-11.

Lee, I.B. 2013. Trend on CFD application in agriculture. Rural Resources 55(1):51-57 (In Korean).

Park, D.Y., S.T. Jang and S.J. Chang. 2013. Numerical study on the thermal environment of a natural light based multi-layered plant factory. J. of Korea Institute of Ecological Architecture and Environment 13(5):43-50 (In Korean).

Park, J.H., J.S. Lee, D.E. Kim and Y.H. Kim. 2011. Analysis of optimum water cooling conditions and heat exchange of LED lamps for plant growth. J. of Biosystems Eng. 36(5):334-341 (In Korean).

Shih, T.H., W.W. Liou, A. Shabbir, Z. Yang and J. Zhu. 1995. A new k-ε eddy viscosity model for high Reynolds number turbulent flows: model development and validation. Computers & Fluids 24(3):227-238.

Yun, H.S., J.K. Kwon, H. Jeong, D.H. Lee, Y.K. Kim and N.K. Yun. 2007. CFD simulation of airflow and heat transfer in the cold container. J. of Biosystems Eng. 32(6): 422-429 (In Korean).

Yun, N.G. 2002. Design and analysis technique for greenhouse environment using CFD simulation. J. of Kor. Res. Soc. Protected Hort. 15(1):20-26 (In Korean).